JOC Article

Electronic Effect on the Kinetics of the Diaza-Cope Rearrangement

Dong-Nam Lee,[†] Hyunwoo Kim,[‡] Leo Mui,[‡] Seung-Woon Myung,[†] Jik Chin,*[,‡] and Hae-Jo Kim*[,†]

Department of Chemistry, College of Natural Sciences, Kyonggi University, Suwon 443-760, Korea, and Department of Chemistry, University of Toronto, 80 St. George Street, Toronto, ON M5S 3H6, Canada

haejkim@kgu.ac.kr; jchin@chem.utoronto.ca

Received January 29, 2009

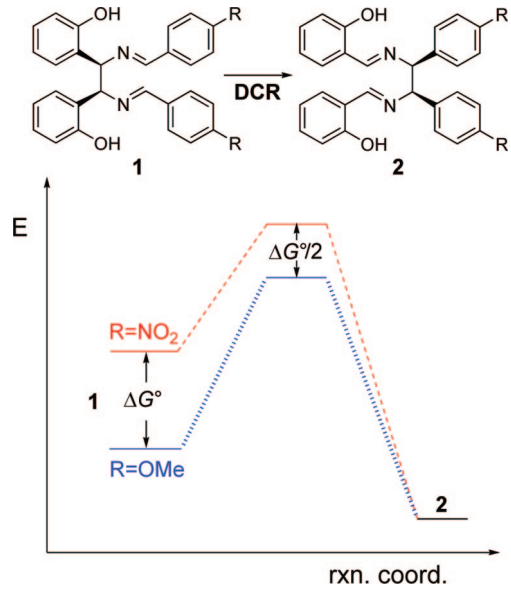

Hammett plot reveals that there is a significant electronic effect on the rate of resonance assisted hydrogen bond (RAHB) directed diaza-Cope rearrangement reaction with a ρ value of 1.6. DFT computation shows that the rearrangement reaction becomes thermodynamically more favorable for the substrates with electron withdrawing substituents. A substrate with the nitro substituent (**1a**) reacts about 50-fold faster than that with the methoxy substituent (**1g**).

Introduction

The resonance assisted hydrogen bond (RAHB)[1] directed diaza-Cope rearrangement (DCR) reaction is of considerable interest for its synthetic applications and mechanistic analysis. The rearrangement reaction has been used to make a variety of *meso*[2] and chiral[3] vicinal diamines that are important as intermediates for making bioactive compounds[4] and stereoselective catalysts.[5] In addition to the practical interest, the diaza-Cope rearrangement reaction represents one of many important [3,3]-sigmatropic reactions including the Cope,[6] Claisen,[7] oxy-Cope,[8] and aza-Cope[9] reactions. Over the years there has been much interest in understanding the mechanism of their reactions. Previously we reported that the two RAHBs in **2** are more stable than the two regular H-bonds in **1** and that the difference in the strength of the H-bonds can be used to direct the diaza-Cope rearrangement to one side.[2b,3c,10] The rearrangement of the *meso* diimine (**1**) is well suited for studying the substitutent effects

* To whom correspondence should be addressed. Phone: +82-31-249-9633. Fax: +82-31-249-9639.
[†] Kyonggi University.
[‡] University of Toronto.

(1) Gilli, P.; Bertolasi, V.; Ferretti, V.; Gilli, G. *J. Am. Chem. Soc.* **2000**, *122*, 10405.

(2) (a) Vögtle, F.; Goldschmitt, E. *Chem. Ber.* **1976**, *109*, 1–40. (b) Chin, J.; Mancin, F.; Thavarajah, N.; Lee, D.; Lough, A.; Chung, D. S. *J. Am. Chem. Soc.* **2003**, *125*, 15276.

(3) (a) Kim, H.-J.; Kim, W.; Lough, A. J.; Kim, B. M.; Chin, J. *J. Am. Chem. Soc.* **2005**, *127*, 16776. (b) Kim, H.-J.; Kim, H.; Alhakimi, G.; Jeong, E. J.; Thavarajah, N.; Studnicki, L.; Koprianiuk, A.; Lough, A. J.; Suh, J.; Chin, J. *J. Am. Chem. Soc.* **2005**, *127*, 16370. (c) Kim, H.; Yen, C.; Preston, P.; Chin, J. *Org. Lett.* **2006**, *8*, 5239. (d) Kim, H.-J.; Chin, J.; Lough, A. J. *Acta Crystallogr.* **2007**, *E63*, o3901.

10.1021/jo900133g CCC: $40.75 © 2009 American Chemical Society
Published on Web 04/01/2009

SCHEME 1. Diaza-Cope Rearrangement for a Series of Diimines

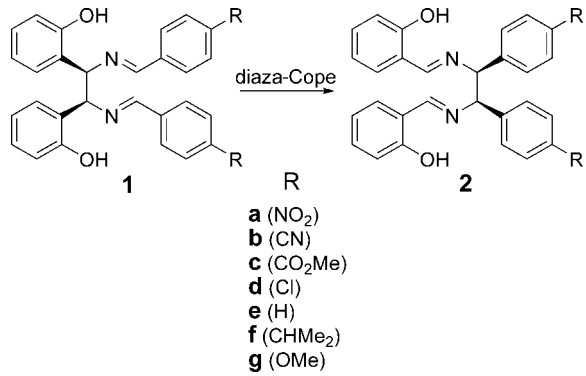

in [3,3]-sigmatropic reactions since the starting materials can be readily prepared from the diamines and aldehydes. Here we report the electronic effect on the rate of the RAHB directed DCR reaction (Scheme 1).

Results and Discussion

NMR Study. To investigate the electronic effect on diaza-Cope rearrangement, we synthesized a series initial diimines (**1a**−**g**) with para substituents that cover a range of Hammett σ_p values.[11] The diimines were prepared by adding 2 equiv of aldehydes to *meso*-1,2-bis(2-hydroxyphenyl)ethylenediamine[12] in methanol at room temperature. The rearrangement reaction of the initial diimine (**1**) to the product diimine (**2**) was monitered by ^{1}H NMR spectroscopy (Figure 1). The phenolic proton signals of **1** were dramatically downfield shifted from 9.7 toward 12.9 ppm while the imine CH protons showed a moderate downfield shift from 8.2 toward 8.5 ppm with the rearrangement reactions (Figure 1), whereas the methine protons were slightly upfield shifted.

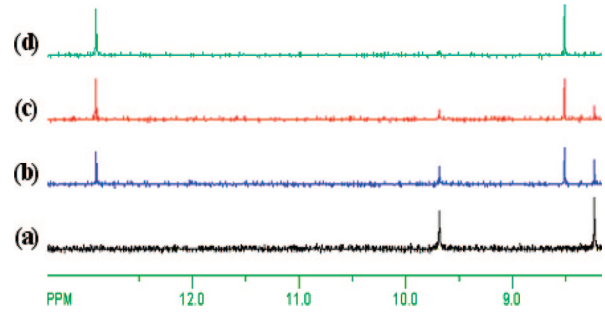

FIGURE 1. Time dependent change in ^{1}H NMR spectra due to the diaza-Cope rearrangement of **1c** in DMSO-d_6 at 25 °C: (a) 0, (b) 15, (c) 23, and (d) 43 h.

TABLE 1. Kinetic Parameters for the Diaza-Cope Rearrangement Reactions[a]

entry	R	σ_p	$10^5 k$ [b] (s^{-1})	$\Delta H^{\ddagger}$ (kcal/mol)	$T\Delta S^{\ddagger}$ [c] (kcal/mol)	$\Delta G^{\ddagger}$ [c] (kcal/mol)
1	**1a**	0.78	3.63	28.15	4.64	23.51
2	**1b**	0.66	3.35	19.42	−4.27	23.69
3	**1c**	0.45	1.42	28.28	4.15	24.13
4	**1d**	0.23	4.34×10^{-1}	30.06	5.23	24.83
5	**1e**	0	1.94×10^{-1}	25.13	−0.13	25.26
6	**1f**	−0.15	2.34×10^{-1}	27.96	2.57	25.39
7	**1g**	−0.27	7.35×10^{-2}	29.93	4.13	25.80

[a] [diimine] = 20 mM in DMSO-d_6. [b] Rate constant at 25 °C. [c] Energy at 25 °C.

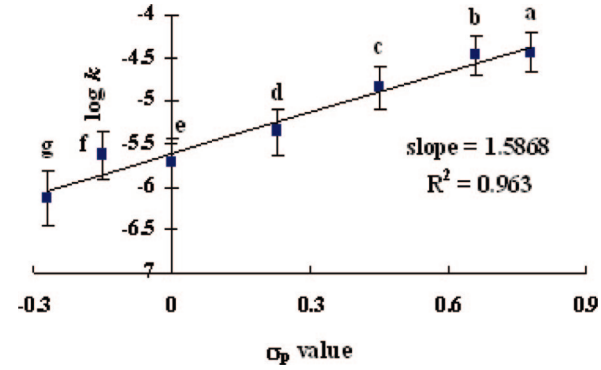

FIGURE 2. The Hammett plot of log k vs. σ_p.

The RAHB directed rearrangement reactions (Scheme 1) went cleanly to completion from the initial *meso*-diimines (**1a**−**g**) to the corresponding product *meso*-diimines (**2a**−**g**).[2a] The first order rate constant for the rearrangement reaction could be obtained from the time dependent changes in the integration values of the imine CH proton signal at various temperatures. The rate constants for the rearrangement reactions were dependent not only on the reaction temperature, but also on the substituents. The rate of the rearrangement reaction increases with increase in electron withdrawing ability of the substituents. Thus the diimine (**1a**) with a highly electron withdrawing substituent rearranges about 50-fold faster than the diimine (**1g**) with an electron donating group (entries 1 vs. 7 in Table 1). The strong electronic effect on the rearrangement reaction can be seen from the slope (ρ = 1.6) of the Hammett plot of log k vs. σ_p (Figure 2).

(4) (a) Gust, R.; Burgermeister, T.; Mannschreck, A.; Schönenberger, H. *J. Med. Chem.* **1990**, *33*, 2535. (b) Bernhardt, G.; Gust, R.; Reile, H.; vom Orde, H.-D.; Müller, R.; Keller, C.; Spruβ, T.; Schönenberger, H.; Burgermeister, T.; Mannschreck, A.; Range, K.-J; Klement, U. *J. Cancer Res. Clin. Oncol.* **1992**, *118*, 201. (c) Gust, R.; Schönenberger, H. *Eur. J. Med. Chem.* **1993**, *28*, 103. (d) Lee, Y.-A; Lee, S. S.; Kim, K. M.; Lee, C. O.; Sohn, Y. S. *J. Med. Chem.* **2000**, *43*, 1409. (e) Vassilev, L. T.; Vu, B. T.; Graves, B.; Carvajal, D.; Podlaski, F.; Filipovic, Z.; Kong, N.; Kammlott, U.; Lukacs, C.; Klein, C.; Fotouhi, N.; Liu, E. A. *Science* **2004**, *303*, 844. (f) Kotti, S. R. S. S.; Timmons, C.; Li, G. *Chem. Biol. Drug Des.* **2006**, *67*, 101.

(5) (a) Kim, H.; So, S. M.; Kim, B. M.; Chin, J. *Aldrichim. Acta* **2008**, *41*, 77. (b) Kim, H.; Nguyen, Y.; Yen, C. P.-H.; Chagal, L.; Lough, A. J.; Kim, B. M.; Chin, J. *J. Am. Chem. Soc.* **2008**, *130*, 12184. (c) Costa, A. M.; Jimeno, C.; Gavenonis, J.; Carroll, P. J.; Walsh, P. J. *J. Am. Chem. Soc.* **2002**, *124*, 6929. (d) Bobb, R.; Alhakimi, G.; Studnicki, L.; Lough, A. J.; Chin, J. *J. Am. Chem. Soc.* **2002**, *124*, 4544. (e) Miller, J. A.; Jin, W.; Nguyen, S. T. *Angew. Chem., Int. Ed.* **2002**, *41*, 2953. (f) Sun, W.; Wang, H.; Xia, C.; Li, J.; Zhao, P. *Angew. Chem., Int. Ed.* **2003**, *42*, 1042. (g) Yoon, T. P.; Jacobsen, E. N. *Science* **2003**, *299*, 1691. (h) Saito, B.; Fu, G. C. *J. Am. Chem. Soc.* **2008**, *130*, 6694. (i) Dai, X.; Strotman, N. A.; Fu, G. C. *J. Am. Chem. Soc.* **2008**, *130*, 3302. (j) Lucet, D.; Le Gall, T.; Mioskowski, C. *Angew. Chem., Int. Ed.* **1998**, *37*, 2580–2627.

(6) (a) Borden, W. T.; Davidson, E. R. *Acc. Chem. Res.* **1996**, *29*, 67–75. (b) Hill, R. K. *Comprehensive Organic Synthesis*; Trost, B. M., Fleming, I., Eds.; Pergamon Press: Oxford, UK, 1991; Vol. 5, p 785.

(7) (a) Ziegler, F. E. *Chem. Rev.* **1988**, *88*, 1423. (b) Wipf, P. *Comprehensive Organic Synthesis*; Trost, B. M., Fleming, I., Eds.; Pergamon Press: Oxford, UK, 1991; Vol. 5, p 827.

(8) (a) Evans, D. A.; Golob, A. M. *J. Am. Chem. Soc.* **1975**, *97*, 4765. (b) Wilson, S. R. *Org. React. (N.Y.)* **1993**, *43*, 93. (c) Paquette, L. A. *Tetrahedron* **1997**, *53*, 13971.

(9) (a) Overman, L. E.; Kakimoto, M.; Okazaki, M. E.; Meier, G. P. *J. Am. Chem. Soc.* **1983**, *105*, 6622. (b) Jacobsen, E. J.; Levin, J.; Overman, L. E. *J. Am. Chem. Soc.* **1988**, *110*, 4329.

(10) Park, H.; Kim, K. M.; Lee, A.; Ham, S.; Nam, W.; Chin, J. *J. Am. Chem. Soc.* **2007**, *129*, 1518.

(11) (a) Hansch, C.; Leo, A.; Taft, R. W. *Chem. Rev.* **1991**, *91*, 165. (b) Dippy, J. F. J.; Williams, F. R. *J. Chem. Soc.* **1934**, 161.

(12) (a) Bryant, C.; Chin, J.; Lough, A. J.; Alhakimi, G. *Acta Crystallogr.* **2002**, *E58*, o456. (b) Voegtle, F.; Goldschmitt, E. *Chem. Ber.* **1976**, *109*, 1–40.

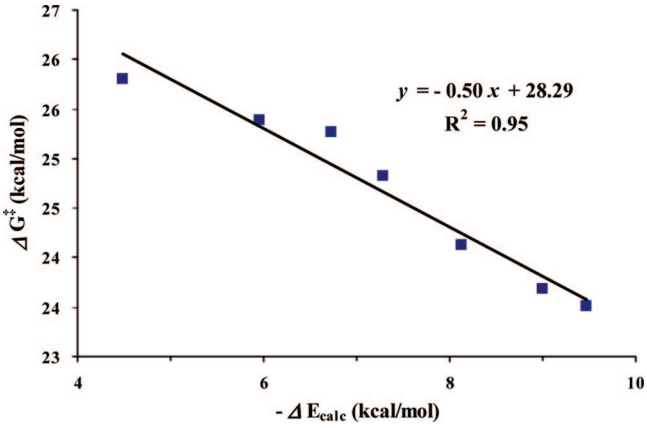

FIGURE 3. Plot of experimental $\Delta G^{\ddagger}$ for the diaza-Cope rearrangement vs. DFT computational energy difference (ΔE) between **1** and **2**.

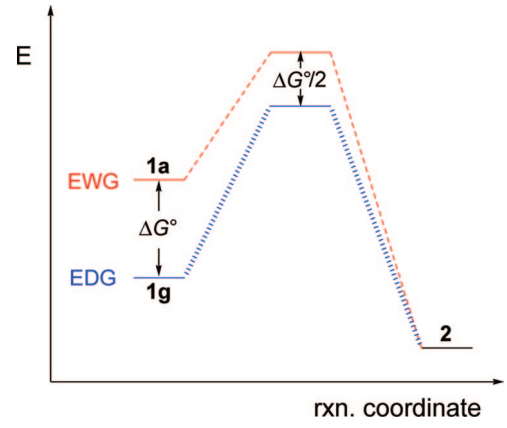

FIGURE 4. Proposed energy profile for the diaza-Cope rearrangement of **1a** and **1g**.

Thermodynamic Parameters Using the Eyring Plot. The activation parameters ($\Delta H^{\ddagger}$and $\Delta S^{\ddagger}$) for the rearrangement of diimines **1** to **2** were obtained from the slopes and intercepts of the Eyring plot (Supporting Information).[13] The rearrangement rates are dominated by the enthalpy of activation ($\Delta H^{\ddagger} \geq 19.4$ kcal/mol) over the entropy of activation ($-4.3 \leq T\Delta S^{\ddagger} \leq 5.2$ kcal/mol at 25 °C). The activation parameters ($\Delta G^{\ddagger}$, $\Delta H^{\ddagger}$, and $\Delta S^{\ddagger}$) for the diaza-Cope rearrangement reactions are summarized in Table 1. The energy barriers ($\Delta G^{\ddagger}$ values in Table 1) for the rearrangement of diimines (**1a**, **1b**) with electron withdrawing groups (nitro, cyano) are low and the reaction takes place rapidly. In contrast, the energy barriers for the rearrangement of diimines (**1f**, **1g**) with electron donating groups are high and the reaction takes place slowly.

The electron donating methoxy substituent is expected to stabilize the starting diimine (**1g**) by conjugation and slow the rearrangement reaction. In contrast, the nitro substituent is expected to destabilize the starting diimine (**1a**) and increase the rearrangement rate. Electronic effects have been shown to be important in other [3,3]-sigmatropic rearrangements including the anionic oxy-Cope[14] and iminium aza-Cope[15] rearrangements.

DFT Computation. In addition to the Hammett plot (Figure 2), it is informative to analyze the electronic effect in the diaza-Cope rearrangement by DFT computation (B3LYP at the 6-31G* level).[16] There is an excellent linear relationship between the experimental energy barrier ($\Delta G^{\ddagger}$ values in Table 1) for the rearrangement reactions and the difference in computed energies of the starting (**1a**−**g**) and product (**2a**−**g**) diimines (Figure 3).

It is interesting that the slope of the plot in Figure 3 is about 0.50, indicating that the electronic effect on the kinetic barrier is half of the electronic effect on the thermodynamic barrier. This is in excellent agreement with the Marcus equation[18] that was originally derived for electron transfer reactions but was also used to analyze proton transfer reactions and other organic reactions.[19] This equation has also been derived from the extended Hammond postulate or the reactivity selectivity principle.[20] According to the Marcus equation (eq 1), the kinetic barrier of a reaction ($\Delta G^{\ddagger}$) is a function of the thermodynamic barrier (ΔG^{0}) and the so-called intrinsic barrier of the reaction ($\Delta G_0^{\ddagger}$) defined as the kinetic barrier in the absence of thermodynamic influence ($\Delta G^{0} = 0$).

$$\Delta G^{\ddagger} = \Delta G_0^{\ddagger}\left(1 + \frac{\Delta G^{0}}{4\Delta G_0^{\ddagger}}\right)^2 \qquad (1)$$

Expansion of eq 1 gives eq 2 with three terms.

$$\Delta G^{\ddagger} = \Delta G_0^{\ddagger} + \frac{\Delta G^{0}}{2} + \frac{(\Delta G^{0})^2}{16\Delta G_0^{\ddagger}} \qquad (2)$$

The last term in eq 2 can be neglected to give eq 3 if the second term is larger ($\Delta G^{0}/2 \gg (\Delta G^{0})^2/16\Delta G_0^{\ddagger}$, thus $8\Delta G_0^{\ddagger} \gg \Delta G^{0}$) as it is in our rearrangement reactions.[21] Equation 3 shows that the change in the kinetic barrier of a reaction is half of the change in the thermodynamic barrier of the reaction (Figure 4). Thus our slope (0.50) in Figure 3 is in accordance with eq 3. Figure 4 shows this relationship in terms of an energy profile for the rearrangement of **1a** and **1g**.

$$\Delta G^{\ddagger} \approx \Delta G_0^{\ddagger} + \frac{\Delta G^{0}}{2} \qquad (3)$$

Conclusion

In conclusion, we synthesized a series of diimines from *meso*-1,2-bis(2-hydroxyphenyl)ethylenediamine and *p*-substituted-benzaldehyde derivatives to investigate the electronic effect on the kinetics of the RAHB directed diaza-Cope

(13) Anslyn, E. V.; Dougherty, D. A. *Modern Physical Organic Chemistry*; University Science Books: Sausalito, CA, 2006; Chapter 7.
(14) (a) Paquette, L. A. *Tetrahedron* **1997**, *53*, 13971. (b) Paquette, L. A.; Reddy, Y. R.; Vayner, G.; Houk, K. N. *J. Am. Chem. Soc.* **2000**, *122*, 10788.
(15) (a) Jacobsen, E. J.; Levin, J.; Overman, L. E. *J. Am. Chem. Soc.* **1988**, *110*, 4329. (b) Fiedler, D.; van Halbeek, H.; Bergman, R. G.; Raymond, K. N. *J. Am. Chem. Soc.* **2006**, *128*, 10240.
(16) Spartan '06 from Wave function Inc. was used for all computations.
(17) Here it is assumed that the changes in entropy for all the rearrangement reactions are comparable in value.
(18) Marcus, R. A. *J. Chem. Phys.* **1956**, *24*, 966–978.
(19) (a) Guthrie, J. P. *J. Am. Chem. Soc.* **2000**, *122*, 5529–5538. (b) Guthrie, J. P.; Pitchko, V. *J. Am. Chem. Soc.* **2000**, *122*, 5520–5528. (c) Guthrie, J. P. *J. Am. Chem. Soc.* **1996**, *118*, 12878–12885. (d) Murdoch, J. R. *J. Am. Chem. Soc.* **1983**, *105*, 2159–2164. (e) Murdoch, J. R. *J. Am. Chem. Soc.* **1983**, *105*, 2660–2667.
(20) Murdoch, J. R. *J. Am. Chem. Soc.* **1972**, *94*, 4410–4418.
(21) In our case, the intrinsic barrier ($\Delta G_0^{\ddagger}$) is more than five times greater than the thermodynamic barrier (ΔG^{0}).

rearrangement reaction. The Hammett plot shows that there is a significant electronic effect for the reaction with a ρ value of 1.6. DFT computation reveals that the rearrangement reaction becomes thermodynamically more favorable for substrates with electron withdrawing substituents. The diimine substrate with a nitro substitutent (**1a**) rearranges about 50 times faster ($\Delta\Delta G^{\ddagger} = -2.3$ kcal/mol) than the one with a methoxy substituent (**1g**) at room temperature. In addition, the electronic effect measured from the experimental kinetic barriers is about half of the electronic effect determined from the computed thermodynamic barriers in accord with the Marcus equation. It is interesting that the experimental kinetic data and the DFT computational thermodynamic data can be combined in a meaningful way to confirm that the Marcus equation is applicable in this reaction. An in-depth understanding of the electronic effects on the rate and equilibrium for the rearrangement reaction should be useful for the synthesis of a wide range of diamines.

Experimental Section

General Procedure for the Synthesis of Compounds 1a−g and 2a−g. *meso*-1,2-Bis(2-hydroxylphenyl)ethylenediamine (0.10 mmol) and 2 equiv of *p*-nitrobenzaldehyde (0.20 mmol) were dissolved in 2.0 mL of methanol each. And then the two solutions were mixed and stirred for an hour at room temperature to give initial diimine **1a** as a white precipitate. As a purification process, the solid was filtered, washed with 0.5 mL of methanol, and dried under vacuum as a white solid. Temperature dependent quantitative conversion of **1a** to **2a** was monitored by a nuclear magnetic resonance spectroscopy.

1a: white solid in 70% yield; ^{1}H NMR (DMSO-d_6, 300 MHz, TMS) δ 9.56 (br, 2H), 8.34 (s, 2H), 8.26 (d, J = 8.7 Hz, 4H), 7.91 (d, J = 8.7 Hz, 4H), 7.37 (d, J = 7.2 Hz, 2H), 7.01−6.99 (m, 2H), 6.73−6.71 (m, 4H), 5.42 (s, 2H); ^{13}C NMR (DMSO-d_6, 75 MHz) δ 160.2, 155.6, 149.1, 141.8, 129.7, 129.4, 128.4, 126.5, 124.4, 119.2, 115.8, 73.2.

2a: yellow solid in a quantitative yield; ^{1}H NMR (DMSO-d_6, 300 MHz, TMS) δ 12.69 (br, 2H), 8.54 (s, 2H), 8.21 (d, J = 8.4 Hz, 4H), 7.62 (d, J = 8.4 Hz, 4H), 7.38−7.32 (m, 4H), 6.89−6.87 (m, 4H), 5.38 (s, 2H); ^{13}C NMR (DMSO-d_6, 75 MHz) δ 167.8, 160.4, 147.6, 147.4, 133.5, 132.4, 129.8, 124.0, 119.5, 119.0, 117.0, 76.8; MS (ESI, positive, MeOH) *m/z* calcd for $C_{28}H_{22}N_4O_6$ 510.15, found $[M + H]^+$ 511.30, $[M + Na]^+$ 533.30.

1b: white solid in 75% yield; ^{1}H NMR (DMSO-d_6, 300 MHz, TMS) δ 9.59 (br, 2H), 8.24 (s, 2H), 7.89 (d, J = 8.1 Hz, 4H), 7.81 (d, J = 8.1 Hz, 4H), 7.31 (d, J = 7.5 Hz, 2H), 6.99 (t, J = 7.8 Hz, 2H), 6.71−6.69 (m, 4H), 5.37 (s, 2H); ^{13}C NMR (DMSO-d_6, 75 MHz) δ 160.6, 155.6, 140.1, 133.2, 129.7, 129.0, 128.4, 126.6, 119.1, 119.0, 115.8, 113.5, 73.0.

2b: yellow solid in a quantitative yield; ^{1}H NMR (DMSO-d_6, 300 MHz, TMS) δ 12.87 (br, 2H), 8.50 (s, 2H), 7.82 (d, J = 8.4 Hz, 4H), 7.51 (d, J = 8.4 Hz, 4H), 7.39−7.31 (m, 4H), 6.90−6.86 (m, 4H), 5.27 (s, 2H); ^{13}C NMR (DMSO-d_6, 75 MHz) δ 167.7, 160.4, 145.6, 133.5, 132.8, 132.4, 129.4, 119.5, 119.1, 119.0, 117.0, 111.0, 77.1; MS (ESI, positive, MeOH) *m/z* calcd for $C_{30}H_{22}N_4O_2$ 470.17, found $[M + H]^+$ 471.40, $[M + Na]^+$ 493.40.

1c: white solid in 80% yield; mp rearrange to **2c** from 140 °C, then ends at 198 °C; ^{1}H NMR (DMSO-d_6, 300 MHz, TMS) δ 9.67 (br, 2H), 8.23 (s, 2H), 7.99 (d, J = 8.1 Hz, 4H), 7.80 (d, J = 8.1 Hz, 4H), 7.31 (d, J = 6.9 Hz, 2H), 6.99−6.98 (m, 2H), 6.72−6.69 (m, 4H), 5.36 (s, 2H), 3.86 (s, 6H); ^{13}C NMR (DMSO-d_6, 75 MHz) δ 166.2, 161.1, 155.6, 140.2, 131.9, 129.9, 129.8, 128.6, 128.4, 126.6, 119.1, 115.9, 74.2, 52.8; HRMS (ESI, positive, MeOH) *m/z* calcd for $C_{32}H_{29}N_2O_6$ $[M + H]^+$ 537.2020, found $[M + H]^+$ 537.2009

2c: yellow solid in a quantitative yield; mp 196−198 °C; ^{1}H NMR (DMSO-d_6, 300 MHz, TMS) δ 12.91 (br, 2H), 8.51 (s, 2H), 7.91 (d, J = 8.1 Hz, 4H), 7.46 (d, J = 8.1 Hz, 4H), 7.34−7.30 (m, 4H), 6.88−6.86 (m, 4H), 5.24 (s, 2H), 3.83 (s, 6H); ^{13}C NMR (DMSO-d_6, 75 MHz) δ 167.4, 166.4, 160.5, 145.5, 133.3, 132.4, 129.6, 129.3, 128.8, 119.4, 119.0, 116.9, 77.5, 52.6; MS (ESI, positive, MeOH) *m/z* calcd for $C_{32}H_{28}N_2O_6$ 536.19, found $[M + H]^+$ 537.40, $[M + Na]^+$ 559.40; HRMS (ESI, positive, MeOH) *m/z* calcd for $C_{32}H_{29}N_2O_6$ $[M + H]^+$ 537.2020, found $[M + H]^+$ 537.2026.

1d: white solid in 80% yield; ^{1}H NMR (DMSO-d_6, 300 MHz, TMS) δ 9.76 (br, 2H), 8.13 (s, 2H), 7.66 (d, J = 8.4 Hz, 4H), 7.49 (d, J = 8.4 Hz, 4H), 7.23 (d, J = 6.9 Hz, 2H), 6.99−6.98 (m, 2H), 6.72−6.67 (m, 4H), 5.26 (s, 2H); ^{13}C NMR (DMSO-d_6, 75 MHz) δ 160.8, 155.6, 136.1, 134.9, 130.0, 129.8, 129.3, 128.4, 126.6, 119.0, 115.9, 73.9.

2d: yellow solid in a quantitative yield; ^{1}H NMR (DMSO-d_6, 300 MHz, TMS) δ 13.08 (br, 2H), 8.48 (s, 2H), 7.41−7.27 (m, 12H), 6.88−6.86 (m, 4H), 5.11 (s, 2H); ^{13}C NMR (DMSO-d_6, 75 MHz) δ 167.1, 160.6, 139.2, 133.3, 132.6, 132.4, 130.2, 128.8, 119.4, 119.0, 116.9, 77.1; MS (ESI, positive, MeOH) *m/z* calcd for $C_{28}H_{22}Cl_2N_2O_2$ 488.11, found $[M + H]^+$ 489.30, $[M + Na]^+$ 511.30.

1e: white solid in 68% yield; ^{1}H NMR (DMSO-d_6, 300 MHz, TMS) δ 9.59 (br, 2H), 8.15 (s, 2H), 7.65 (d, J = 7.5 Hz, 4H), 7.44−7.42 (m, 6H), 7.21 (d, J = 6.9 Hz, 2H), 6.99−6.98 (m, 2H), 6.74−6.65 (m, 4H), 5.26 (s, 2H); ^{13}C NMR (DMSO-d_6, 75 MHz) δ 162.1, 155.7, 136.0, 131.5, 129.9, 129.1, 128.4, 128.3, 126.7, 118.9, 116.1, 74.3.

2e: yellow solid in a quantitative yield; ^{1}H NMR (DMSO-d_6, 300 MHz, TMS) δ 13.18 (br, 2H), 8.44 (s, 2H), 7.33−7.20 (m, 12H), 6.86−6.83 (m, 6H), 5.07 (s, 2H); ^{13}C NMR (DMSO-d_6, 75 MHz) δ 166.7, 160.6, 140.5, 133.1, 132.3, 128.8, 128.4, 128.0, 119.2, 119.0, 116.9, 78.2; MS (ESI, positive, MeOH) *m/z* calcd for $C_{28}H_{24}N_2O_2$ 420.18, found $[M + H]^+$ 421.40, $[M + Na]^+$ 443.40.

1f: white solid in 85% yield; mp rearrange to **2f** from 143 °C, then ends at 198 °C; ^{1}H NMR (DMSO-d_6, 300 MHz, TMS) δ 10.01 (br, 2H), 8.10 (s, 2H), 7.57 (d, J = 8.1 Hz, 4H), 7.29 (d, J = 8.1 Hz, 4H), 7.16 (d, J = 6.9 Hz, 2H), 6.99−6.98 (m, 2H), 6.73−6.64 (m, 4H), 5.20 (s, 2H), 2.98−2.78 (m, 2H), 1.20 (d, J = 6.9 Hz, 12H); ^{13}C NMR (DMSO-d_6, 75 MHz) δ 161.9, 155.8, 152.2, 133.8, 129.9, 128.6, 128.3, 127.2, 126.7, 118.9, 116.1, 74.6, 33.9, 24.1; HRMS (ESI, positive, MeOH) *m/z* calcd for $C_{34}H_{37}N_2O_2$ $[M + H]^+$ 505.2849, found $[M + H]^+$ 505.2847

2f: yellow solid in a quantitative yield; mp 196−198 °C; ^{1}H NMR (DMSO-d_6, 300 MHz, TMS) δ 13.23 (br, 2H), 8.38 (s, 2H), 7.29−7.14 (m, 12H), 6.85−6.81 (m, 4H), 4.99 (s, 2H), 2.96−2.76 (m, 2H), 1.14 (d, J = 6.9 Hz, 12H); ^{13}C NMR (DMSO-d_6, 75 MHz) δ 166.5, 160.6, 148.0, 138.1, 133.0, 132.2, 128.3, 126.7, 119.2, 119.0, 116.8, 77.9, 33.4, 24.3; MS (ESI, positive, MeOH) *m/z* calcd for $C_{34}H_{36}N_2O_2$ 504.28, found $[M + H]^+$ 505.50, $[M + Na]^+$ 531.50; HRMS (ESI, positive, MeOH) *m/z* calcd for $C_{34}H_{37}N_2O_2$ $[M + H]^+$ 505.2849, found $[M + H]^+$ 505.2839.

1g: white solid in 74% yield; ^{1}H NMR (DMSO-d_6, 300 MHz, TMS) δ 10.05 (br, 2H), 8.03 (s, 2H), 7.59 (d, J = 8.1 Hz, 4H), 7.12 (d, J = 6.9 Hz, 2H), 6.99−6.97 (m, 6H), 6.72−6.61 (m, 4H), 5.13 (s, 2H), 3.78 (s, 6H); ^{13}C NMR (DMSO-d_6, 75 MHz) δ 162.1, 161.4, 155.8, 130.2, 129.9, 128.7, 128.3, 126.8, 118.9, 116.1, 114.6, 74.9, 55.8.

2g: yellow solid in a quantitative yield; ^{1}H NMR (DMSO-d_6, 300 MHz, TMS) δ 13.26 (br, 2H), 8.43 (s, 2H), 7.32−7.23 (m, 8H), 6.89−6.82 (m, 8H), 4.99 (s, 2H), 3.69 (s, 6H); ^{13}C NMR (DMSO-d_6, 75 MHz) δ 166.3, 160.7, 158.9, 133.0, 132.6, 132.2, 129.5, 119.2, 119.1, 116.9, 114.2, 77.5, 55.5; MS (ESI, positive, MeOH) *m/z* calcd for $C_{30}H_{28}N_2O_4$ 480.20, found $[M + H]^+$ 481.40, $[M + Na]^+$ 517.50.

Acknowledgment. We thank to Kyonggi University of Korea (KGU-2006-007), 2008 Kyonggi University Specialization Program, and the Natural Sciences and Engineering Research Council of Canada for financial support. The authors also are grateful to the Department of Chemistry, Seoul National University, Korea, for free access to the NMR facility.

Supporting Information Available: Detailed description of experimental and NMR/mass data for **1** and **2**, and first-order kinetic plots for **1**. This material is available free of charge via the Internet at http://pubs.acs.org.

JO900133G